Clinica Chimica Acta 475 (2017) 91–96

Contents lists available at ScienceDirect

Clinica Chimica Acta

journal homepage: www.elsevier.com/locate/cca

Application of digital PCR with chip-in-a-tube format to analyze *Adenomatous polyposis coli* (*APC*) somatic mosaicism

Tomoaki Kahyo[a,*,1], Moriya Iwaizumi[b,2], Hidetaka Yamada[a], Hong Tao[a], Kiyotaka Kurachi[c], Haruhiko Sugimura[a,*,1]

[a] Department of Tumor Pathology, Hamamatsu University School of Medicine, 1-20-1 Handayama, Hamamatsu, Shizuoka 431-3192, Japan
[b] First Department of Medicine, Hamamatsu University School of Medicine, 1-20-1 Handayama, Hamamatsu, Shizuoka 431-3192, Japan
[c] Second Department of Surgery, Hamamatsu University School of Medicine, 1-20-1 Handayama, Hamamatsu, Shizuoka 431-3192, Japan

ARTICLE INFO

Keywords:
dPCR
Mosaicism
APC genetic analysis

ABSTRACT

Background: Over the past decade, digital PCR (dPCR) technology has significantly improved, and its application in clinical diagnostics is rapidly advancing. The Clarity™ dPCR platform, which employs the chip-in-a-tube format to broaden its range of applications, has been used to determine gene copy number. However, detection of mutations in human samples, the most demanding task in clinical practice, has not yet been reported using this platform.

Methods: The Clarity™ dPCR platform was used to detect somatic *Adenomatous polyposis coli* mosaicism c.834 + 2 T > C, which had been identified using next-generation sequencing (NGS) technology in a patient with sporadic familial adenomatous polyposis. In addition, we were able to determine the size of the dPCR product.

Results: The mutation rate in the peripheral blood of the patient calculated using the dPCR platform was 13.2%. This was similar to that determined using NGS (12.7%). In contrast, in healthy donors, the mutation rate was < 0.1%. Furthermore, it was confirmed that the dPCR product size was consistent with its theoretical value.

Conclusion: Our results show that the dPCR platform with the chip-in-a-tube format is suitable for the analysis of mosaicism and enables the validation of the dPCR product size.

1. Introduction

Digital PCR (dPCR) enables the absolute quantitation of DNA in a reaction mixture and is considered to be one of the most effective molecular diagnostic tools [1]. The basic concept of dPCR was first described in 1992 [2], and the term "digital PCR" was first used in 1999 [3]. A situation wherein DNA templates are absent or present as a single molecule per partition can be created by diluting DNA templates and dividing them into partitions. After PCR, the amplified fluorescent signal in each partition is determined as negative or positive, and their proportions are determined. The target copy number is calculated using positive proportion based on Poisson statistics.

Partitioning techniques of commercially available dPCR platforms are roughly categorized into two types: droplet-based and chip-based partitioning. In the former, DNA templates are divided into water-in-oil droplets using microfluidics and proprietary surfactants [4,5]. In the latter, DNA templates are divided into tens of thousands of partitions on a chip using microfluidics [6]. Key features of dPCR systems are their sensitivity, accuracy, productivity, broad utility, usability, and cost. Through optimization of these aspects, dPCR technologies have impacted medical studies, such as detection of copy number alteration, base substitution using liquid biopsy in oncology [7–9], and highly precise virus detection in infectious diseases [10,11]. Therefore, dPCR technologies are being recognized as next-generation molecular diagnostic tools.

In our previous report, we identified a novel somatic *Adenomatous polyposis coli* (*APC*) mosaicism corresponding to a splice donor site in a patient with sporadic familial adenomatous polyposis using next-generation sequencing (NGS) technology [12]. The aim of this study was to investigate whether the latest dPCR platform in which DNA templates are distributed by capillary action into partitions on chips built into PCR tubes [13] is useful for the detection of somatic *APC* mosaicism.

* Corresponding authors.
E-mail addresses: kahyo@hama-med.ac.jp (T. Kahyo), hsugimur@hama-med.ac.jp (H. Sugimura).
[1] Double corresponding authors.
[2] Present address: Department of Laboratory Medicine, Hamamatsu University School of Medicine, 1-20-1 Handayama, Hamamatsu, Shizuoka 431-3192, Japan.

http://dx.doi.org/10.1016/j.cca.2017.10.015
Received 31 August 2017; Received in revised form 18 October 2017; Accepted 18 October 2017
Available online 18 October 2017

2. Materials and methods

2.1. Patients

A 40-year-old male (AGFAP001-1) visited the Hamamatsu University Hospital owing to the result of a fecal occult blood examination for colorectal cancer. Upon endoscopic examination, several colorectal adenomatous polyps and fundic gland polyposis were identified [12]. Peripheral blood samples were collected from the proband and his parents (father, AGFAP001-2; mother, AGFAP001-3). Peripheral blood samples from a donor population aged ≥ 60 years were collected in the Iwata City Hospital [14]. The design of this study was approved by the Institutional Review Boards of Hamamatsu University School of Medicine (G-260-4), and written informed consent was obtained from the patient and his parents.

2.2. DNA extraction

Genomic DNA was extracted from peripheral blood samples using the QIAamp DNA Blood Maxi Kit (Qiagen, Valencia, CA, USA). Subsequently, it was subjected to genomic DNA screen tape assay using 2200 TapeStation system (Agilent Technologies, Santa Clara, CA, USA) to determine the amount of genomic DNA (> 200 bp) and the DNA integrity number (DIN).

2.3. Digital PCR

Reaction mixtures (total volume = 15 μL) were prepared with 1 × PCR Master mix (JN Medsys, Singapore), 1 × JN solution (JN Medsys, Singapore), 10–20 ng of genomic DNA (3 μL), 1 pmol each of Locked Nucleic Acid (LNA) probes modified using HEX™ and FAM™ fluorescent dyes (LNA PrimeTime®, Integrated DNA Technologies, Coralville, IA, USA), and 0.5 pmol each of forward and reverse primers (5′-GGTCAAGGAGTGGGAGAAATC-3′ and 5′-TCTTAGAACCATCTTGCT TCATACT-3′, respectively). Detailed information on LNA probes is shown in Fig. 2A. Melting temperature values of LNA probes were calculated using the supplier tool (http://biophysics.idtdna.com/) under the following conditions: 50 mM Na^+/K^+, 0.80 mM dNTPs, 66.6 nM oligonucleotides, and 3 mM Mg^{2+}. Sample partitioning and fluorescence detection were performed using the Clarity™ dPCR system (JN Medsys) [13]. The reaction mixture was loaded onto a chip with an auto loader, and partitions were sealed using a sealing enhancer and 230 μL of a proprietary sealing fluid. Thermal cycling was performed under the following conditions: 95 °C for 5 min, 42 cycles of 95 °C for 50 s and 58 °C for 90 s, and 70 °C for 5 min. Ramp rate was set to 1 °C/s (Life Eco, Bioer Technology, Hangzhou, China). Fluorescent signals of HEX™ and FAM™ were detected using the Clarity™ reader, and the obtained data were analyzed using the Clarity™ software (ver. 2.0), which determines the DNA copy number according to Poisson statistics. The mean of triplicate assays was calculated in each experiment; the final mean value and relative standard deviation (RSD) was obtained from three independent experiments (Table 1). RSD was expressed using the following formula: standard deviation/mean. Mutation rate (%) was calculated using the following formula: $C_{mut} / (C_{ref} + C_{mut}) \times 100$, where C_{ref} and C_{mut} are copy numbers of the reference and mutant alleles, respectively. For the calculation of a detection limit, C_{ref} and C_{mut} were measured using a dilution series of AGFAP001-1 genomic DNA (0.11–0.45 ng) mixed with AGFAP001-2 genomic DNA (10.3 ng) (Fig. 3). The assays were repeated 20 times. The maximally diluted point at which the mean − 3 × standard deviation (SD) of C_{mut} was greater than the mean + 3 × SD of C_{mut} for AGFAP001-2 was determined as the detection limit of mutation rate (%).

2.4. Collection of PCR products

To collect digital PCR products from the chips built in PCR tubes, sealing fluid was removed from the tube, and 100 μL of TE buffer (10 mM Tris-HCl, pH 8.0; 0.1 mM EDTA) was added. After vigorous vortexing for 30 s, the solution was transferred to another tube and concentrated by the ethanol precipitation method. To assess PCR product size, one chip equivalent of concentrated solution was subjected to the High Sensitivity D1000 screen tape assay (Agilent Technologies).

3. Results

3.1. Digital PCR with the chip-in-a-tube format

To generate robust data, it is essential to fully understand the nature of the technical platform used. In the Clarity™ dPCR platform, high density partitions (> 10,000) are crafted on a chip built into a 0.2-mL 8-strip PCR tube (Fig. 1A, I) [13]. After preparing the reaction mixture, it was loaded onto the chip using an autoloader device (Fig. 1A, II). To avoid cross-contamination between partitions, the chips were sealed using a sealing enhancer and proprietary sealing fluid (Fig. 1A, III, and IV). Eight chip dPCR reactions (8-tube PCR strip) were simultaneously conducted following the above described steps (II–IV). The PCR was performed using a conventional thermal cycler (Fig. 1A, V), and fluorescent signals were detected using the Clarity™ reader (Fig. 1A, VI). The procedure took < 4 h in total. Fluorescent signals on the chip were imaged as shown in Fig. 1B, wherein positive and negative partitions are displayed as yellow and blue dots, respectively. Positive and negative partitions indicate the presence and absence of a target region, respectively. Black background corresponds to the partitions that did not receive any reaction mixture. Therefore, in most cases, the whole image of the fluorescent signals is shaped like the chip. The Clarity™ dPCR platform is adjusted such that at least 10,000 partitions are filled with the reaction mixture. In the present study, 95.5% of the experiments had a frequency of > 10,000 total signal counts per assay (Fig. 1C).

3.2. Dual LNA probe assay by the Clarity™ dPCR platform

The Clarity™ dPCR platform for life science research has been used in four previous studies [13,15–17] that investigated gene copy number. However, mutation detection in human samples has not yet been reported. We have previously identified a novel somatic *APC* mosaicism corresponding to the splice donor site (c.834 + 2 T > C) from a patient with sporadic familial adenomatous polyposis using NGS technology [12]. To investigate whether the Clarity™ dPCR platform can be used to detect a gene mutation in human samples, we used the platform to validate *APC* mosaic mutations. Fluorescent probes containing LNAs, known to bind to complementary target molecules with very high affinity, were designed for the reference (T) and mutation (C) alleles (Fig. 2A) [18]. FAM™ emission is detected when the DNA template with the mutant allele is present in a partition, whereas HEX™ emission is detected in the case of the reference allele. As a result, HEX™ and FAM™ emissions were detected in a large number of partitions in the peripheral blood genomic DNA of the patient when compared with the no-template control (NTC) (Fig. 2B). However, only HEX™ emission was detected from a large number of partitions in the control paternal sample. Positive partitions were distributed throughout the chip indicating that loading and sealing procedures were effective (Fig. 2C). Copy numbers of the reference and mutation sites were determined on the basis of Poisson statistics, and the mutation rate was calculated (Table 1). The mutation rate calculated from the patient's genomic DNA was 13.2%, which was similar to that calculated by NGS (12.7%).The mutation rates calculated from the patient's parents and healthy donors genomic DNA were < 0.1%. Detection limit for the *APC* c.834 + 2 T > C mutation site was calculated as 0.298% using diluted

Table 1
Mutation rate calculated by the Clarity™ digital PCR platform.

Sample[a]	Tissue	Input DNA (ng)	DIN[b]	Iwaizumi M. et al[c]	This study (by digital PCR)[d]			
				Mutation rate by NGS (%)	Mutation (copies)	Reference (copies)	Mutation rate (%)	
							Mean	RSD
NTC	–	–	–	–	1.23	0.00	N/A	N/A
AGFAP001-1	Blood	11.3	7.6	12.7	379	2.48×10^3	13.2	0.0353
AGFAP001-2	Blood	10.3	7.7	0.0167	1.08	3.42×10^3	0.0341	0.439
AGFAP001-3	Blood	10.8	7.6	0.0136	0.956	3.04×10^3	0.0313	0.637
Donor-1	Blood	11.7	7.3	–	1.64	3.01×10^3	0.0543	0.414
Donor-2	Blood	10.5	7.6	–	1.06	2.90×10^3	0.0406	0.539
Donor-3	Blood	17.6	7.9	–	4.24	5.65×10^3	0.0713	0.783
Donor-4	Blood	12.3	7.6	–	2.38	4.16×10^3	0.0666	0.557
Donor-5	Blood	19.2	7.0	–	1.48	6.79×10^3	0.0213	0.571
Donor-6	Blood	14.4	6.7	–	3.44	4.67×10^3	0.0728	0.729

[a] NTC, no-template control; AGFAP001-1, proband; AGFAP001-2, father; AGFAP001-3, mother; donor, healthy donor.
[b] DIN, DNA integrity number.
[c] [12].
[d] Experiments were run in triplicates and independently repeated three times; data are expressed as the mean value; RSD, relative standard deviation; N/A, not applicable.

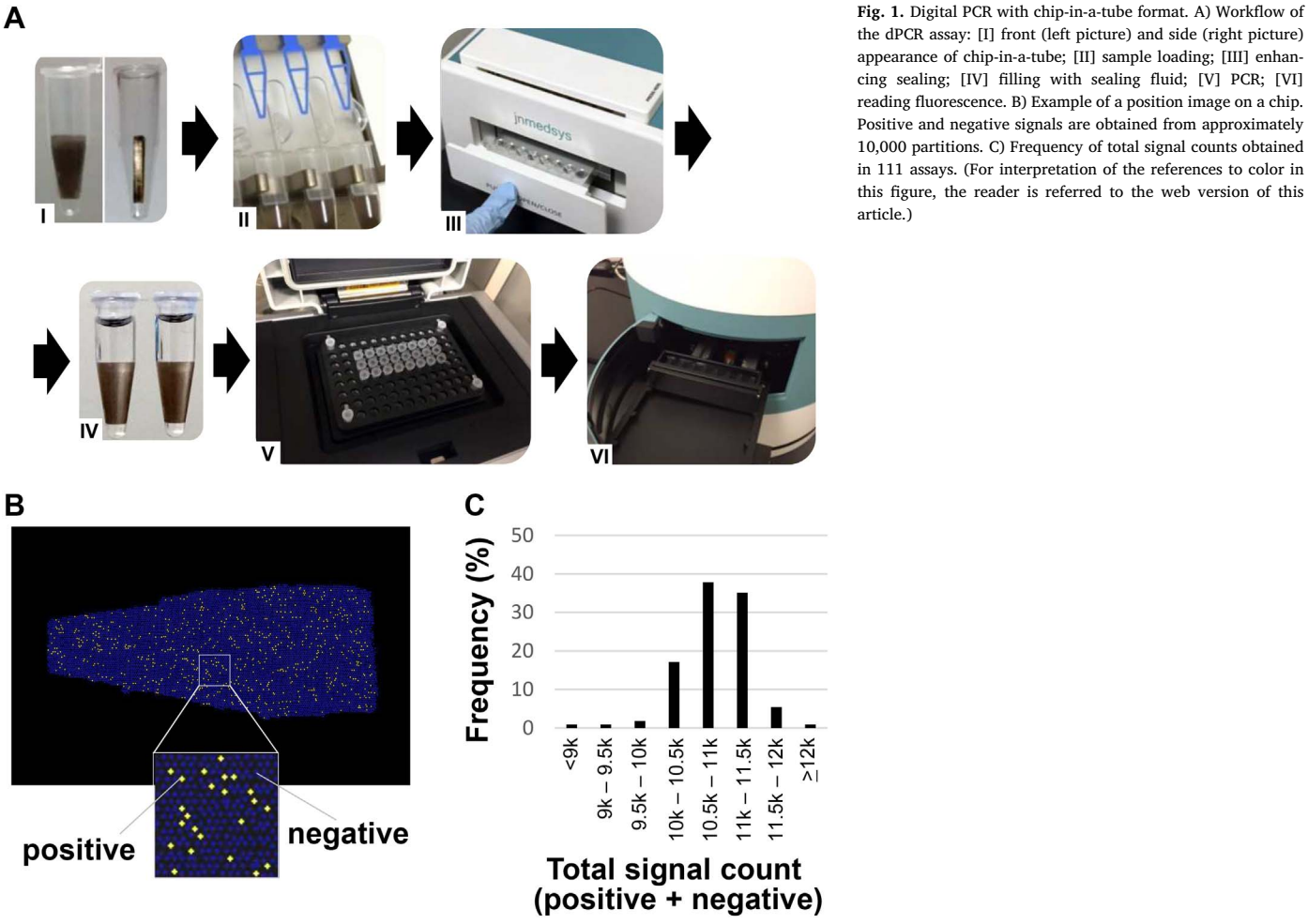

Fig. 1. Digital PCR with chip-in-a-tube format. A) Workflow of the dPCR assay: [I] front (left picture) and side (right picture) appearance of chip-in-a-tube; [II] sample loading; [III] enhancing sealing; [IV] filling with sealing fluid; [V] PCR; [VI] reading fluorescence. B) Example of a position image on a chip. Positive and negative signals are obtained from approximately 10,000 partitions. C) Frequency of total signal counts obtained in 111 assays. (For interpretation of the references to color in this figure, the reader is referred to the web version of this article.)

AGFAP001-1 genomic DNA mixed with AGFAP001-2 genomic DNA (10–11 ng/assay) (Fig. 3).

3.3. Collection of dPCR products

Before performing the dPCR assay, a conventional PCR was performed to confirm that the *APC* target site product was amplified as a single, visible band and that the size was consistent with its theoretical value (data not shown). It is unusual to collect dPCR products from partitions and evaluate them after performing a dPCR assay because existing dPCR platforms are not designed for subsequent collection of dPCR products. Although the sealing principle of the Clarity™ dPCR platform is not completely disclosed by the manufacturer, we assumed that the proprietary sealing fluid was not hardened as in the droplet dPCR platform and that the partitioned area on the chip was not irreversibly closed. Therefore, we explored the possibility of collecting

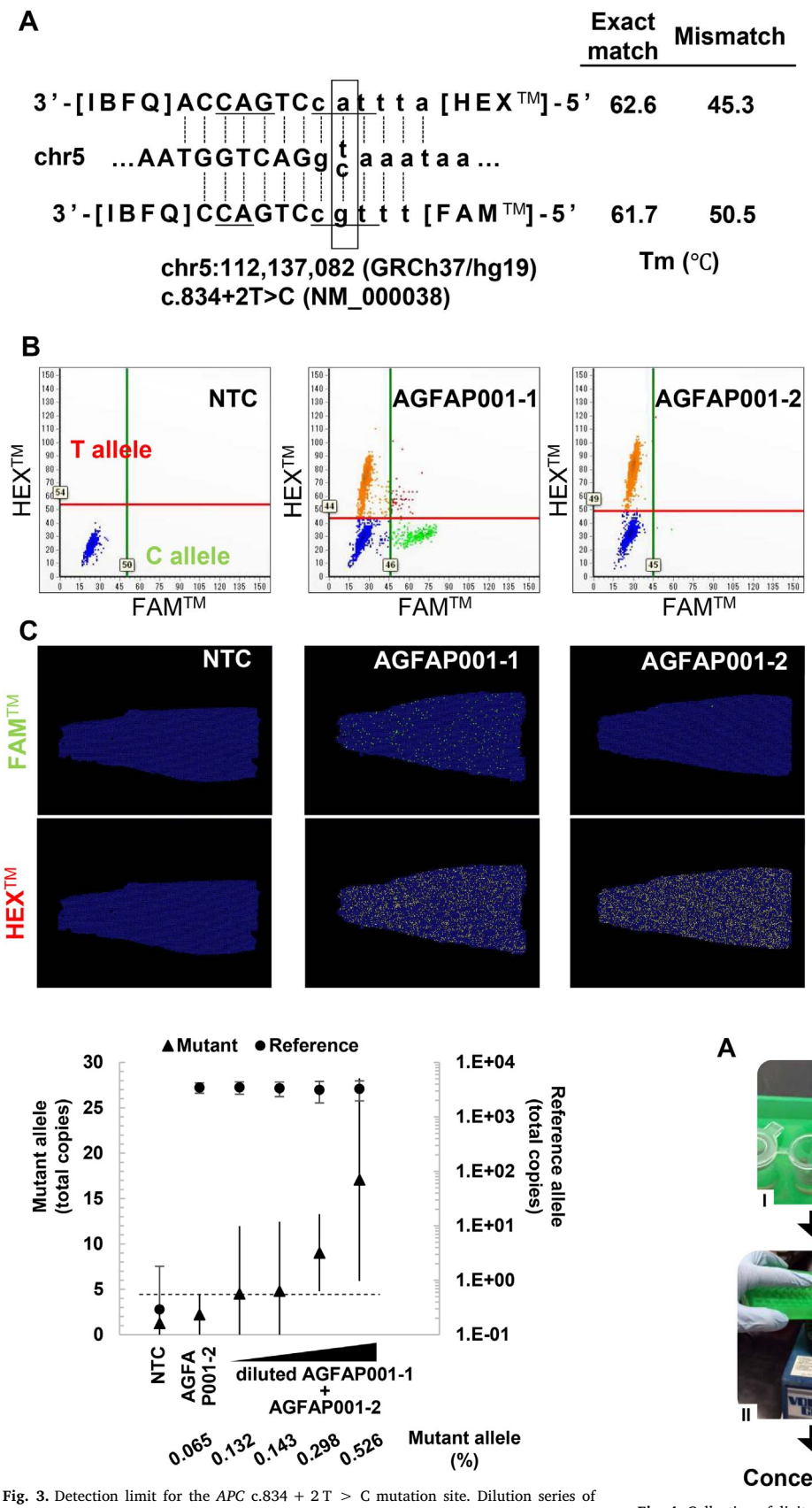

Fig. 2. Dual LNA probe assay by the Clarity™ digital PCR platform. A) LNA probe design for the *APC* c.834 + 2 T > C mutation site. The capital and lower case letters indicate exon and intron sequences of *APC* gene, respectively. Underlined letters show Locked Nucleic Acids (LNA). IBFQ (Iowa Black®) is a quencher. HEX™ and FAM™ are fluorescent dyes. Indicated melting temperature (Tm) values were calculated with 66.6 nM probe. B) Scatter plot of HEX™ (T allele) and FAM™ (C allele). NTC, AGFAP001-1, and AGFAP001-2 are no-template control, proband, and healthy father of the proband, respectively. C) Position images of HEX™ and FAM™.

Fig. 3. Detection limit for the *APC* c.834 + 2 T > C mutation site. Dilution series of AGFAP001-1 genomic DNA were mixed with AGFAP001-2 genomic DNA, and the copy numbers of the mutant (C) and reference (T) alleles were measured. The total amount of genomic DNA was 10–11 ng/assay, and the assays were repeated 20 times. Error bars show 3 × standard dilutions (SD), and the dashed line shows the mean + 3 × SD of the mutant allele copy number for AGFAP001-2. NTC, no-template control.

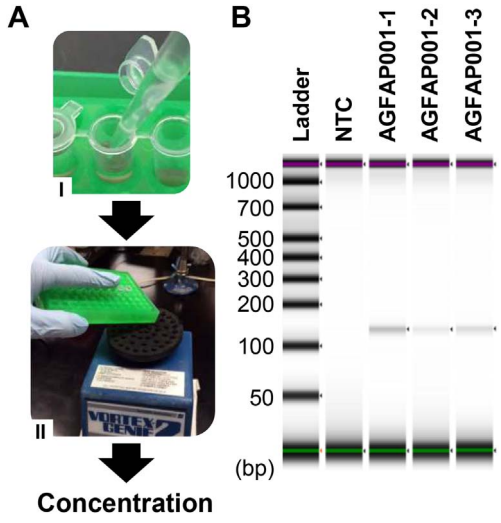

Fig. 4. Collection of digital PCR products. A) The workflow to collect the dPCR products: [I] removing oil of the measured chip-in-a-tube and adding TE buffer; [II] vigorously vortexing. B) Concentrated dPCR products were subjected to the electrophoresis. Predicted target size is 123 bp. NTC, no-template control.

dPCR products of the *APC* target site using the chip-in-a-tube. To achieve this, the sealing fluid was removed from the assay tubes followed by the addition of Tris-HCl buffer (Fig. 4A). The samples were vigorously vortexed and the solution was then transferred to new tubes and concentrated. The concentrated solution, equivalent to one chip, was subjected to microfluidic electrophoresis (Fig. 4B), which showed that the dPCR product was amplified as a single, visible band and that its size was consistent with the predicted value (123 bp).

4. Discussion

The Clarity™ dPCR platform employs the chip-in-a-tube format with a universal 8-strip PCR tube, which enables high-throughput dPCR assays and can be handled in the same manner as conventional PCR assays. This dPCR platform has been used for the quantitation of viruses and bacteria in circulating cell-free samples and wastewater treatment plants [15–17]. In this study, we confirmed that the Clarity™ dPCR platform could also be used to detect gene mutations in human samples, which, combined with the high-throughput capacity of dPCR, are encouraging for its future applications in clinical diagnosis alongside conventional PCR.

dPCR assays have been previously used to validate mutant alleles identified by NGS and array methods in mosaicism studies [19–21]. In the present study, the applicability of the Clarity™ platform for dPCR was evaluated, and the mutation rate of *APC* c.834 + 2 T > C in the patient's peripheral blood genomic DNA was found to be similar to that determined by NGS. The detection limit for the *APC* c.834 + 2 T > C mutation site was calculated to be 0.298% using 10–11 ng of genomic DNA. The results suggest that the *APC* mosaic mutation could be validated at the level of ≥ 9 copies/1500 diploid cells by the Clarity™ dPCR platform using peripheral blood samples. Mutation rates in blood samples from the patient's parents calculated using dPCR assays were slightly higher than those calculated using NGS. However, they still were < 0.1% similar to other healthy donors. A small number of the mutant alleles (false positives) were detected in the patient's parents and healthy donors. Because the copy number of the reference allele was hardly detected in NTC (mean copy number < 1, Table 1 and Fig. 3), in-laboratory contamination of samples is unlikely to cause false positives. Unknown DNA sources containing sequences that preferentially hybridize to the mutant allele probe may be a reason for the false positives. However, mutation rates measured in the parents and healthy donors (shown in Table 1) are similar to the mutation rates indicated in the previous study of droplet dPCR assays with healthy donors [22]. Further adjustments of probe design and thermal cycling conditions may be required to decrease false positives in addition to preventing DNA contamination.

dPCR has often been compared with quantitative real-time PCR (qPCR), and the strengths of dPCR, such as high accuracy and sensitivity, have been highlighted. However, the collection of dPCR products has not been suggested as a routine part of the assay, particularly in commercially available dPCR platforms. However, it is common to discuss melting curve analysis and electrophoresis of PCR products in conventional qPCR assays. For the Clarity™ dPCR platform, we found that dPCR products can be readily collected from chips after the assay and subjected to electrophoresis for size confirmation. This collection step is more crucial in intercalator-based assays than in fluorescence probe assays. Availability of such a collection procedure is also expected from other dPCR platforms.

5. Conclusion

The Clarity™ dPCR platform with the chip-in-a-tube format is suitable for the detection of *APC* mosaicism c.834 + 2 T > C in peripheral blood genomic DNA samples, and it allows for the collection of dPCR products from the assay tubes. These findings may help the implementation of clinical diagnosis using dPCR.

Funding sources

This study was supported by a Grant-in-Aid for Scientific Research (C) from JSPS to T.K. (No. 15K08397) and M.I. (No. 16K0930501), and by grants from AMED (No. 927960719), Grant-in-Aid for Exploratory Research (No. 16K15256), and Expenditure for Associated Projects of Incentive Special Budget for the Promotion of National University Reform in Management Expenses Grants (No. 1019253) to H.S. The funders had no role in the study design, data collection, and analysis; decision to publish; or preparation of the manuscript.

Competing interests

The authors declare that they have no competing interests.

Acknowledgments

We thank Dr. Sato (Hamamatsu University School of Medicine) for collecting the donor blood samples.

References

[1] J.F. Huggett, S. Cowen, C.A. Foy, Considerations for digital PCR as an accurate molecular diagnostic tool, Clin. Chem. 61 (1) (2015) 79–88.
[2] P.J. Sykes, S.H. Neoh, M.J. Brisco, E. Hughes, J. Condon, A.A. Morley, Quantitation of targets for PCR by use of limiting dilution, BioTechniques 13 (3) (1992) 444–449.
[3] B. Vogelstein, K.W. Kinzler, P.C.R. Digital, Proc. Natl. Acad. Sci. U. S. A. 96 (16) (1999) 9236–9241.
[4] M.M. Kiss, L. Ortoleva-Donnelly, N.R. Beer, J. Warner, C.G. Bailey, B.W. Colston, J.M. Rothberg, D.R. Link, J.H. Leamon, High-throughput quantitative polymerase chain reaction in picoliter droplets, Anal. Chem. 80 (23) (2008) 8975–8981.
[5] B.J. Hindson, K.D. Ness, D.A. Masquelier, P. Belgrader, N.J. Heredia, A.J. Makarewicz, I.J. Bright, M.Y. Lucero, A.L. Hiddessen, T.C. Legler, T.K. Kitano, M.R. Hodel, J.F. Petersen, P.W. Wyatt, E.R. Steenblock, P.H. Shah, L.J. Bousse, C.B. Troup, J.C. Mellen, D.K. Wittmann, N.G. Erndt, T.H. Cauley, R.T. Koehler, A.P. So, S. Dube, K.A. Rose, L. Montesclaros, S. Wang, D.P. Stumbo, S.P. Hodges, S. Romine, F.P. Milanovich, H.E. White, J.F. Regan, G.A. Karlin-Neumann, C.M. Hindson, S. Saxonov, B.W. Colston, High-throughput droplet digital PCR system for absolute quantitation of DNA copy number, Anal. Chem. 83 (22) (2011) 8604–8610.
[6] E.A. Ottesen, J.W. Hong, S.R. Quake, J.R. Leadbetter, Microfluidic digital PCR enables multigene analysis of individual environmental bacteria, Science 314 (5804) (2006) 1464–1467.
[7] H. Gevensleben, I. Garcia-Murillas, M.K. Graeser, G. Schiavon, P. Osin, M. Parton, I.E. Smith, A. Ashworth, N.C. Turner, Noninvasive detection of HER2 amplification with plasma DNA digital PCR, Clin. Cancer Res. 19 (12) (2013) 3276–3284.
[8] P. Laurent-Puig, D. Pekin, C. Normand, S.K. Kotsopoulos, P. Nizard, K. Perez-Toralla, R. Rowell, J. Olson, P. Srinivasan, D. Le Corre, T. Hor, Z. El Harrak, X. Li, D.R. Link, O. Bouché, J.F. Emile, B. Landi, V. Boige, J.B. Hutchison, V. Taly, Clinical relevance of KRAS-mutated subclones detected with picodroplet digital PCR in advanced colorectal cancer treated with anti-EGFR therapy, Clin. Cancer Res. 21 (5) (2015) 1087–1097.
[9] X. Li, Y. Liu, W. Shi, H. Xu, H. Hu, Z. Dong, G. Zhu, Y. Sun, B. Liu, H. Gao, C. Tang, X. Liu, Droplet digital PCR improved the EGFR mutation diagnosis with pleural fluid samples in non-small-cell lung cancer patients, Clin. Chim. Acta 471 (2017) 177–184.
[10] M.C. Strain, S.M. Lada, T. Luong, S.E. Rought, S. Gianella, V.H. Terry, C.A. Spina, C.H. Woelk, D.D. Richman, Highly precise measurement of HIV DNA by droplet digital PCR, PLoS One 8 (4) (2013) e55943.
[11] R.T. Hayden, Z. Gu, J. Ingersoll, D. Abdul-Ali, L. Shi, S. Pounds, A.M. Caliendo, Comparison of droplet digital PCR to real-time PCR for quantitative detection of cytomegalovirus, J. Clin. Microbiol. 51 (2) (2013) 540–546.
[12] M. Iwaizumi, H. Tao, K. Yamaguchi, H. Yamada, K. Shinmura, T. Kahyo, Y. Yamanaka, K. Kurachi, K. Sugimoto, Y. Furukawa, H. Sugimura, A novel APC mosaicism in a patient with familial adenomatous polyposis, Hum. Genome Var. 2 (2015) 15057.
[13] H. Low, S.J. Chan, G.H. Soo, B. Ling, E.L. Tan, Clarity™ digital PCR system: a novel platform for absolute quantification of nucleic acids, Anal. Bioanal. Chem. 409 (7) (2017) 1869–1875.
[14] H. Tao, K. Shinmura, M. Suzuki, S. Kono, R. Mibu, M. Tanaka, Y. Kakeji, Y. Maehara, T. Okamura, K. Ikejiri, K. Futami, Y. Yasunami, T. Maekawa, K. Takenaka, H. Ichimiya, N. Imaizumi, H. Sugimura, Association between genetic polymorphisms of the base excision repair gene MUTYH and increased colorectal cancer risk in a Japanese population, Cancer Sci. 99 (2) (2008) 355–360.
[15] J.H. Vo, W.L. Nei, M. Hu, W.M. Phyo, F. Wang, K.W. Fong, T. Tan, Y.L. Soong, S.L. Cheah, K. Sommat, H. Low, B. Ling, J. Ng, W.L. Tan, K.S. Chan, L. Oon, J.Y. Ying, M.H. Tan, Comparison of circulating tumour cells and circulating cell-free Epstein-Barr virus DNA in patients with nasopharyngeal carcinoma undergoing radiotherapy, Sci Rep 6 (1) (2016) 13.

[16] M. Harb, P.Y. Hong, Molecular-based detection of potentially pathogenic bacteria in membrane bioreactor (MBR) systems treating municipal wastewater: a case study, Environ. Sci. Pollut. Res. Int. 24 (6) (2017) 5370–5380.
[17] J.R. Muhammad, H.A. Nur, S. Poorani, H. Colin, C.R. Rita, H. Pei-Ying, Membrane Bioreactor-based Wastewater Treatment Plant in Saudi Arabia: Reduction of Viral Diversity, Load, and Infectious Capacity, 9 (2017), p. 534.
[18] A. Simeonov, T.T. Nikiforov, Single nucleotide polymorphism genotyping using short, fluorescently labeled locked nucleic acid (LNA) probes and fluorescence polarization detection, Nucleic Acids Res. 30 (17) (2002) e91.
[19] I.M. Campbell, B. Yuan, C. Robberecht, R. Pfundt, P. Szafranski, M.E. McEntagart, S.C. Nagamani, A. Erez, M. Bartnik, B. Wiśniowiecka-Kowalnik, K.S. Plunkett, A.N. Pursley, S.H. Kang, W. Bi, S.R. Lalani, C.A. Bacino, M. Vast, K. Marks, M. Patton, P. Olofsson, A. Patel, J.A. Veltman, S.W. Cheung, C.A. Shaw, L.E. Vissers, J.R. Vermeesch, J.R. Lupski, P. Stankiewicz, Parental somatic mosaicism is under-recognized and influences recurrence risk of genomic disorders, Am. J. Hum. Genet. 95 (2) (2014) 173–182.
[20] X. Xu, X. Yang, Q. Wu, A. Liu, A.Y. Ye, A.Y. Huang, J. Li, M. Wang, Z. Yu, S. Wang, Z. Zhang, X. Wu, L. Wei, Y. Zhang, Amplicon resequencing identified parental mosaicism for approximately 10% of “de novo” SCN1A mutations in children with Dravet syndrome, Hum. Mutat. 36 (9) (2015) 861–872.
[21] A.F. Daly, B. Yuan, F. Fina, J.H. Caberg, G. Trivellin, L. Rostomyan, W.W. de Herder, L.A. Naves, D. Metzger, T. Cuny, W. Rabl, N. Shah, M.L. Jaffrain-Rea, M.C. Zatelli, F.R. Faucz, E. Castermans, I. Nanni-Metellus, M. Lodish, A. Muhammad, L. Palmeira, I. Potorac, G. Mantovani, S.J. Neggers, M. Klein, A. Barlier, P. Liu, L. Ouafik, V. Bours, J.R. Lupski, C.A. Stratakis, A. Beckers, Somatic mosaicism underlies X-linked acrogigantism syndrome in sporadic male subjects, Endocr. Relat. Cancer 23 (4) (2016) 221–233.
[22] D. Sefrioui, A. Perdrix, N. Sarafan-Vasseur, C. Dolfus, A. Dujon, J.M. Picquenot, J. Delacour, M. Cornic, E. Bohers, M. Leheurteur, O. Rigal, I. Tennevet, J.C. Thery, C. Alexandru, C. Guillemet, C. Moldovan, C. Veyret, T. Frebourg, F. Di Fiore, F. Clatot, Short report: monitoring ESR1 mutations by circulating tumor DNA in aromatase inhibitor resistant metastatic breast cancer, Int. J. Cancer 137 (10) (2015) 2513–2519.